Tissue spreading on implantable substrates is a competitive outcome of cell–cell vs. cell–substratum adhesivity

Peter L. Ryan*†, Ramsey A. Foty*‡, Joachim Kohn†, and Malcolm S. Steinberg*§

*Department of Molecular Biology, Princeton University, Princeton, NJ 08544; and †Department of Chemistry, Rutgers University, Piscataway, NJ 08854

Communicated by Robert Langer, Massachusetts Institute of Technology, Cambridge, MA, December 20, 2000 (received for review September 12, 2000)

While the interactions of cells with polymeric substrata are widely studied, the influence of cell–cell cohesivity on tissue spreading has not been rigorously investigated. Here we demonstrate that the rate of tissue spreading over a two-dimensional substratum reflects a competition or "tug-of-war" between cell–cell and cell–substratum adhesions. We have generated both a "library" of structurally related copolymeric substrata varying in their adhesivity to cells and a library of genetically engineered cell populations varying only in cohesivity. Cell–substratum adhesivity was varied through the poly(ethylene glycol) content of a series of copolymeric substrata, whereas cell–cell cohesivity was varied through the expression of the homophilic cohesion molecules N- and R-cadherin by otherwise noncohesive L929 cells. In the key experiment, multicellular aggregates containing about 600 cells were allowed to spread onto copolymeric surfaces. We compared the spreading behavior of aggregates having different levels of cell–cell cohesivity on a series of copolymeric substrata having different levels of cell–substratum adhesivity. In these experiments, cell–cell cohesivity was measured by tissue surface tensiometry, and cell–substratum adhesivity was assessed by a distractive method. Tissue spreading was assayed by confocal microscopy as the rate of cell emigration from similar-sized, fluorescence-labeled, multicellular aggregates deposited on each of the substrata. We demonstrate that either decreasing substratum adhesivity or increasing cell–cell cohesivity dramatically slowed the spreading rate of cell aggregates.

Tissue spreading over a substratum is a fundamental process in animal development, wound healing, and malignancy. Understanding the process of tissue spreading is critically important for the emerging field of tissue engineering and for the future use of biomaterials scaffolds for tissue or organ regeneration. Because spreading of a three-dimensional tissue over a surface must come at the expense of associations between cells, greater cell–cell cohesivity should restrain cell emigration (1). Evaluating the expectation that tissue spreading involves a competition between cell–cell and cell–substratum attachments requires the isolation of these two variables from all others. Toward that end, a "library" of four cell lines identical except in their cadherin expression and consequently in their cohesivity has been generated. To vary the cell–substratum adhesivity, a library of six structurally related copolymers differing in poly(ethylene glycol) (PEG) content has been prepared. We then compared the adhesion-related behavior of each of these cell populations on each of these substrata.

Materials and Methods

Reagents. DMEM, antibiotics (penicillin-streptomycin, gentamycin, G418) and culture supplements (sodium pyruvate; nonessential amino acids, L-glutamine) were purchased from BRL Products (Life Technologies, Gaithersburg, MD). FBS was obtained from HyClone. Fibronectin, laminin, trypsin-EDTA, and PKH2 green fluorescent cell linker kit were supplied by Sigma. Calcein acetoxymethyl ester (calcein Am) was obtained from Molecular Probes.

Substrata. Synthesis and characterization of poly(desamino-tyrosyl-tyrosine ethyl ester [DTE] carbonate), poly (DTE carbonate), and an array of copolymers with similar structure and bulk properties, poly(DTE-co-PEG carbonate) incorporating (1–5%) of PEG blocks with molecular weight of 1,000 g/mole (Fig. 1) have been described (2–5). For cell attachment and spreading analysis, 96-well polypropylene plates were coated with 100-μl aliquots of 2% solutions of each polymer in methylene chloride and allowed to evaporate to dryness in a sterile flow hood. When dry, plates were sealed and stored at 4°C. For aggregate spreading assays, polymers were spin-coated onto clean, 15-mm circular glass coverslips and placed in 24-well polystyrene plates (Falcon 1147) or mounted on glass slides. Fibronectin-coated (10 mg/ml), laminin-coated (10 mg/ml), and untreated glass coverslips served as control substrata.

Cells. The R-cadherin-transfected L cell line (6, 7) LR1 was obtained from L. Reichardt (University of California, San Francisco). A total of 2×10^6 originally noncohesive embryonic mouse L929 fibroblasts (L cells) were transfected by electroporation in 400 μl transfection medium (RPMI 1640, 1% dextrose, 1 mM β-mercaptoethanol) with 40 μg pMiwcN chicken N-cadherin (8) expression vector (9). pwlneo (GIBCO) was included for G418 selection. Transfected cells were diluted 1/100 and placed in medium containing 800 μg/ml G418 (GIBCO). Resistant cells were grown to confluence, detached by trypsin/Ca^{2+} treatment, and stained with an anti-chicken N-cadherin antibody (NCD2, Zymed) on ice for 45 min. After several washes in Hanks' balanced salt solution, cells were mixed with a fluorescein isothiocyanate-conjugated secondary antibody and placed on ice for 30 min. N-cadherin-expressing cells were then autocloned into 96-well plates by using the CloneCyt Integrated Deposition System (Becton-Dickinson Immunocytometry Systems). Positive clones were reanalyzed by FACS, and two L cell lines, LN2 and LN5, expressing different levels of N-cadherin were propagated for these studies.

Cell Culture. Cells were cultured at 37°C under 95% air/5% CO_2 in DMEM containing 100 units/ml penicillin, 100 μg/ml streptomycin, 10 μg/ml gentamycin, and 10% FBS. Cells were maintained in 200 μg/ml G418.

Cell Attachment and Spreading Assays. Flat-bottom, 96-well polypropylene microplates (Phenix Research Products, Hayward, CA) were used, black plates for the cell attachment assays,

Abbreviations: DTE, desamino-tyrosyl-tyrosine ethyl ester; PEG, poly(ethylene glycol).

See commentary on page 4282.

†Present address: Department of Animal and Dairy Sciences and College of Veterinary Medicine, Mississippi State University, Mississippi State, MS 39762.

‡Present address: Department of Surgery, Robert Wood Johnson Medical School, New Brunswick, NJ 08903.

§To whom reprint requests should be addressed. E-mail: msteinberg@princeton.edu.

The publication costs of this article were defrayed in part by page charge payment. This article must therefore be hereby marked "*advertisement*" in accordance with 18 U.S.C. §1734 solely to indicate this fact.

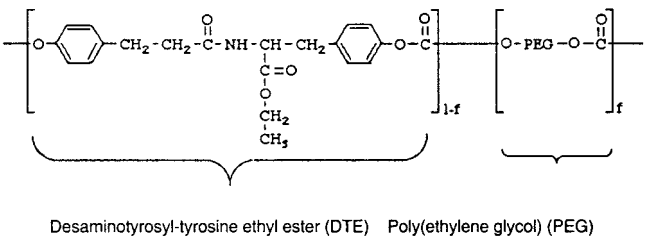

Fig. 1. Variations in the molar fraction f of PEG present in copolymers of DTE and PEG make it possible to modulate the adhesivity of the polymer surface to cells by changing the amount and conformation of serum proteins adsorbed onto the polymer surface. Molecular weight of PEG: 1,000 g/mole; molecular weight of the copolymers varied from about 70,000 to 100,000 g/mole. With increasing f, the copolymer surface becomes more hydrophilic, as indicated by a decrease in the air-water contact angle (2).

and transparent plates for the cell spreading assays. On each plate, six columns of wells were coated with the polymers, ranging from 0 to 5% PEG in 1% increments. Before use, these wells were filled with 10% FBS. The uncoated wells in the seventh column were filled with 1% BSA solution, and wells in the eighth column were left untreated. FBS and BSA solutions were aspirated and the wells were thoroughly rinsed before use, A single-cell suspension was prepared by trypsin/EDTA treatment. Cells then were labeled with the fluorogenic dye calcein AM according to the manufacturer's instructions. Wells of both black and transparent plates were seeded in duplicate with 100 μl of a cell suspension (0.5×10^6 cells/ml), and the plates were incubated under cell culture conditions for 2, 6, 12, and 24 h. At each time point, plates were removed, and each well was filled with medium, sealed with adhesive film (LMT-Seal-Ex; Phenix Research Products), and inverted for 5 min, permitting unattached cells to fall away. Sealing film was then removed, and the plates were blotted on paper towels to remove excess liquid. Plates were gently washed with medium, and excess liquid was removed as described above. Two hundred microliters PBS containing 1 mM Ca^{2+} then was added to each well. Rate of cell attachment was determined with a fluorescence microplate reader (absorbance maximum 494 nm, emission maximum 517 nm; Cytofluor 4000 Plate Reader, Perkin–Elmer Biosystems. Cell spreading was observed by phase-contrast microscopy and recorded ($\times$20 objective) by using National Institutes of Health IMAGE. Each experiment was repeated at least three times.

Cell Aggregate Production. Upon reaching confluency, cells were dissociated with 0.05% trypsin/0.53 mM EDTA and washed in complete medium to inhibit trypsin. Cells were resuspended at 10^6 cells/ml. Three milliliters was transferred to a 10-ml round-bottomed flask (Bellco Glass). Flasks were placed in a G76 gyratory shaker bath (New Brunswick Scientific) at 37°C, 95% air/5% CO_2 for 24–48 h at 120 rpm. Under these conditions, aggregates 30–150 μm in diameter were formed in suspension and a thin ribbon of aggregated cells formed at the flask-air-medium interface. The suspended aggregates were collected for aggregate spreading assays. For tissue surface tension analysis, 1-mm^2 fragments were cut with microscalpels from the thin ribbon of aggregated cells. These were transferred to a fresh flask and incubated under the same conditions for 24–48 h or until they formed spheroids.

Aggregate Spreading Assay. Cells were stained with PKH2 green fluorescent membrane intercalating dye before aggregate formation, following the manufacturer's instructions. Cell viability was confirmed by using Trypan blue dye exclusion. Aggregates $\approx$80–100 μm in diameter, each containing $\approx$600 cells, were placed on polymer-coated glass coverslips previously attached to chamber slides, which were sealed with a glass coverslip ringed with silicone lubricant grease and cultured under conditions described above. Confocal imaging was performed with a Bio-Rad MRC600 scan head mounted on a Nikon Optiphot II microscope. Images were collected with a $\times$20 Plan Apochromatic 0.75 NA objective by using the 488-nm line of an argon/krypton laser for fluorochrome excitation. Kalman-averaged (n = 4) optical sections of spreading cell aggregates ($\times$20 objective) were obtained at 2, 8, and 24 h.

Aggregate Cohesivity Measurement. Aggregate cohesivity was measured under tissue culture conditions via the equilibrium force exerted by the aggregate on parallel compressing plates, which prevent it from rounding up, constraining it to a subspherical shape. From this force and the aggregate's geometry, both measured at no fewer than two different equilibrium forces and shapes, the aggregate's cohesivity was computed, as its surface tension, through the Young-Laplace equation as described (10–12).

Serum Dependence of Aggregate Spreading. PKH2-labeled cell aggregates of low cohesivity (LN2 cells, 1.9 dyne/cm) were placed on poly(DTE-carbonate) and cultured for 24 h in medium supplemented with either 10% FBS or 2% TCM serum substitute (Celox, Hopkins, MN). Images were recorded as described above.

Results

Aggregates of LR1, LN5, and LN2 cells, transfected to express cadherins, were found to possess levels of cohesivity that differ significantly among the three cell lines. LR1 aggregates were the most cohesive, with a surface tension of 8.7 $\pm$ 0.4 dyne/cm. LN5 aggregates were intermediate in cohesivity, with a surface tension of 3.1 $\pm$ 0.2 dyne/cm. LN2 aggregates were the least cohesive, with a surface tension of 1.9 $\pm$ 0.2 dyne/cm. The parent cell line, L-929, does not aggregate and therefore its cohesivity approaches zero.

In the poly(DTE-co-PEG carbonate) polymers, PEG incorporation resulted in a change from a highly adhesive (PEG content = 0 mol %) to a minimally adhesive substratum (PEG content = 5 mol %). Cell adhesivity to the polymers was monitored by two criteria: the rate of cell attachment and the degree of cell spreading over time. Rate of attachment of all four L cell lines markedly declined with increasing PEG content of the polymer substrata. This was evident at all time points examined and is illustrated after 24 h in Fig. 2. Cell population spreading was also markedly reduced by increasing PEG content of the polymer substrata (Fig. 3, top to bottom). The reduction in adhesivity was most marked in both assays as PEG content exceeded 3%. Cadherin-expressing cells seeded on the 5% PEG substratum tended to aggregate rather than spread and in all cases were easily removed upon gentle washing of the plate. Observed in all cell lines, this is illustrated for lines LN5 and LR1 in Fig. 3, in which it is also seen that cells displaying different cadherins may differ in their culture morphology, LN5 cells adopting a rounder shape on the substratum than LR1 cells.

To evaluate the effects of both substratum adhesivity and aggregate cohesivity upon the rate of aggregate spreading, small, spheroidal aggregates of similar size, composed of cadherin-expressing L cells, were placed on polymer-coated coverslips and cultured (Fig. 4). These aggregates spread by the emigration of cells onto the substratum, emigration being maximal on the 0% PEG-containing polymer, decreasing with increasing PEG content and approaching zero on the 5% PEG-containing polymer. For example, averaged over 24 h, the rate of spreading of LN2 aggregates, with a cohesivity of 1.9 dyne/cm, was decreased from 6,814 μm^2/h to 4,176 μm^2/h to 651 μm^2/h by increasing the PEG content of the copolymer from 0% to 3% to 5%, respectively

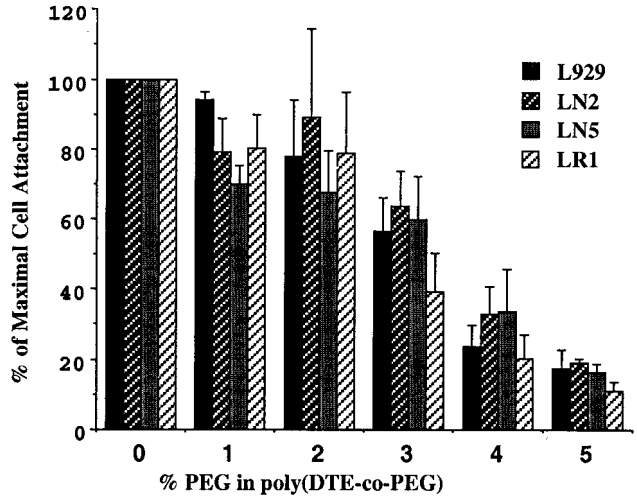

Fig. 2. Quantitative analysis of single cell attachment on poly(DTE-co-PEG carbonate) substrata shows that in all L cell types, rate of attachment markedly declined with increasing PEG content. Fluorescence-labeled (calcein-AM dye) single cell suspensions of low, intermediate, and high cohesivity were allowed to attach for 24 h on polymeric substrata containing 0–5% PEG. Rate of cell attachment was measured as fluorescence intensity at each time point. Data points represent averages of measurements made in duplicate and repeated at least three times.

(Fig. 4 *A–C*). For LN5 aggregates, with a cohesivity of 3.1 dyne/cm, the rates of spreading on the polymers containing 0% and 3% PEG were 3,612 μm^2/h and 1,841 μm^2/h, respectively (Fig. 4 *D* and *E*). These aggregates spread little or not at all on the polymer containing 5% PEG (Fig. 4 *C* and *F*). This demonstrates that at constant cell–cell cohesivity, diminishing cell–substratum adhesivity, within the range tested, leads to slower rates of tissue spreading over the substratum.

Of particular interest, the rate of aggregate spreading on a given substratum was strongly influenced by the intensity of cohesion among the spreading cells themselves. Cadherin-transfected L cell aggregates with lower cohesivity spread faster on each substratum than those of higher cohesivity. For example, on the copolymer containing 3% PEG, increasing aggregate cohesivity from 1.9 to 3.1 dyne/cm reduced the average spreading rate from 4,176 μm^2/h to 1,841 μm^2/h (Fig. 4 *B* and *E*). This effect was so great that aggregates of the most cohesive kind (LR1; 8.7 dyne/cm) hardly spread at all even on that substratum to which their individual cells adhered most strongly (Fig. 4 *G–I*). The same trends were observed on fibronectin- and laminin-coated substrata (data not shown). Thus a competition exists between cell–substratum adhesivity, which promotes the exchange of cell–cell for cell–substratum adhesions, and cell–cell cohesivity, which opposes this exchange.

To determine whether the effects of polymer PEG content upon cell and aggregate attachment and spreading are due to direct cell-polymer interactions or are mediated by components deposited upon the polymer from the serum in the culture medium, PKH2-labeled cell aggregates of low cohesivity (LN2 cells, 1.9 dyne/cm) were cultured for 24 h on poly(DTE-carbonate) in medium supplemented with either 10% FBS or TCM, a commercial serum substitute. In the presence of serum, cells emigrated from the aggregates, completely dispersing in 24 h, while in the absence of serum, no cell emigration occurred, even on this most-preferred substratum surface (Fig. 5).

Discussion

The physical competition demonstrated here between cell–cell and cell–substratum adhesions was postulated many years ago

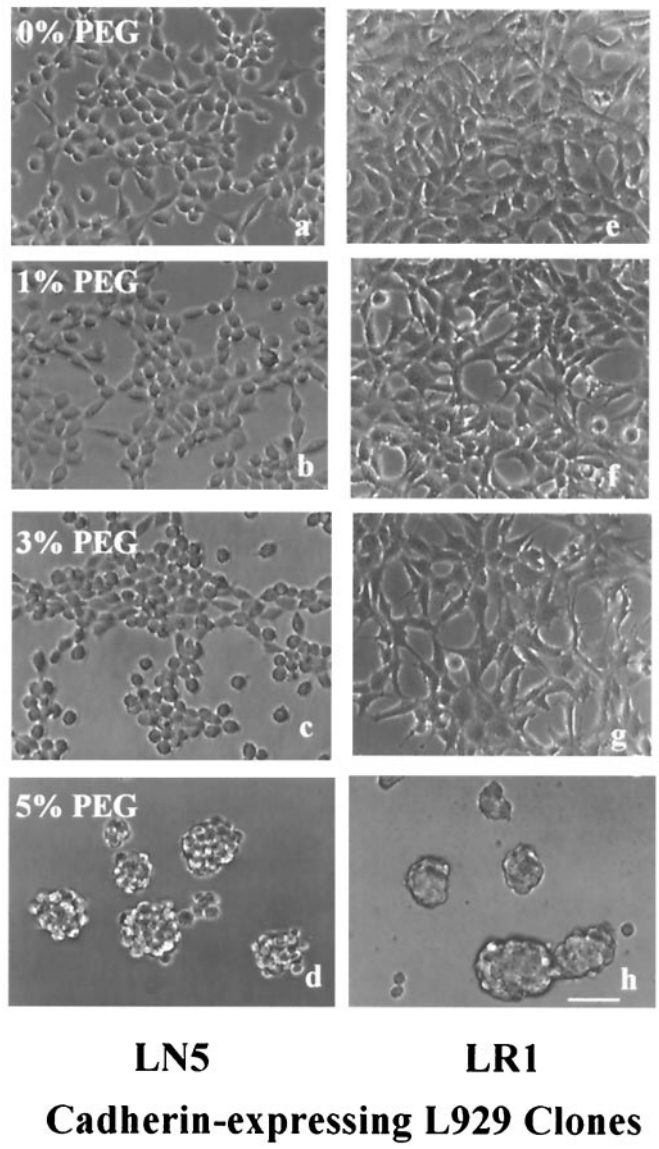

Fig. 3. At a constant level of cell–cell adhesion, cell population spreading on poly(DTE-co-PEG carbonate) substrates depends on the adhesivity of the substratum. Single cell suspensions of all L cell types, exemplified here by LN5 (*a–d*) and LR1 (*e–h*) were allowed to attach for 24 h to polymeric substrata containing 0–5% PEG. Note cadherin-specific differences in culture morphology. In all cases, cell population spreading was markedly reduced by increased PEG content of the substratum (top to bottom). Cells seeded on the substratum of highest PEG content tended to aggregate on the substratum, from which the aggregates were easily removed by gentle agitation. (Scale bar = 100 μm.)

(1). However, its empirical demonstration had to await the development of a means for measuring the cohesive intensities of cell aggregates (13), the production of a set of cell populations differing in this single property, and the synthesis of a library of copolymeric substrata whose surface composition could be gradually changed to provide different levels of cell–substratum adhesivity without introducing significant changes in polymer bulk structure or properties (2). As reported earlier by Tziampazis *et al.* (14) the incorporation of small amounts of PEG into the structure of poly(DTE carbonate) can modulate the attachment, adhesion strength, and motility of L929 fibroblasts due to the ability of PEG to modulate the amounts and conformations of serum proteins adsorbed onto the polymer surface. These

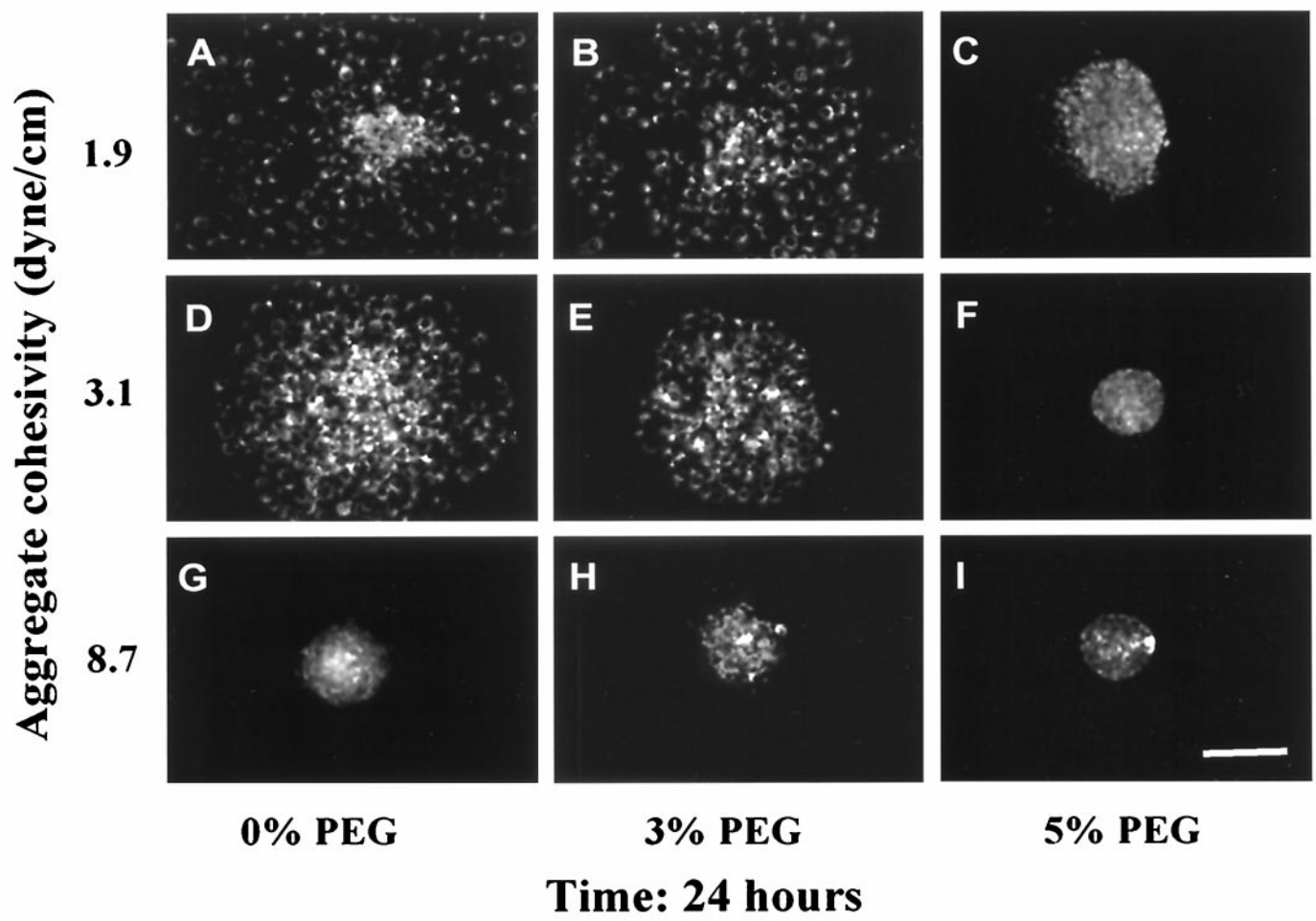

Fig. 4. Matrix of results showing the interplay between cell–cell cohesivity and cell–substratum adhesivity. Increasing cell–cell cohesivity decreases aggregate spreading rate whereas increasing cell–substratum adhesivity increases aggregate spreading rate. Small, fluorescence-labeled cell aggregates of low, intermediate, and high cohesivity (top to bottom) were allowed to spread for 24 h on polymeric substrata containing 0%, 3%, and 5% PEG (left to right). The most cohesive aggregates hardly spread at all on even the most adhesive substratum (*G*) and even the least cohesive aggregates were unable to spread significantly on the least adhesive substratum (*C*). (Scale bar = 100 μm.)

observations are in agreement with our finding that the spreading of cell aggregates upon poly(DTE carbonate) occurs in the presence of serum but not in its absence and supports our suggestion that PEG content modulates cell adhesion to poly(DTE-co-PEG carbonate) by regulating the polymer's avidity for cell-binding serum proteins such as fibronectin and/or vitronectin.

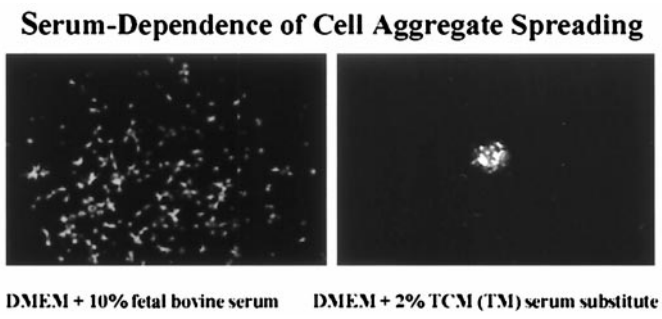

Fig. 5. Serum-derived proteins mediate cell aggregate spreading. PKH2 fluorescence-labeled cell aggregates of low cohesivity (LN2 cells, 1.9 dyne/cm) were deposited and cultured for 24 h on a poly(DTE-carbonate)-coated surface in medium containing 10% FBS (*Left*) or TCM (TM) serum substitute (*Right*). Cells emigrated rapidly in the presence of serum but not at all in its absence.

The hypothesis addressed here is a thermodynamic hypothesis based on the relative free energies of cell–cell and cell–substratum binding. Rigorous testing of this hypothesis would require thermodynamic measurements of these binding energies. Commonly, however, other kinds of measurements are used as surrogates for thermodynamic ones. Distractive measurements (e.g., refs. 15–17) of the peak force required to separate cohering cells suffer from their sensitivity to such properties as cell plasticity and to the manner in which the force is applied; nor is the fracture plane necessarily that of cell–cell contact (18, 19). Kinetic measurements of cell–cell adhesiveness via the rates of initiation of adhesions between cells (e.g., refs. 20–22) do not reflect the great strengthening of cell adhesions that occurs after cell–cell adhesions are initiated (e.g., ref. 17), nor do reaction rates in general necessarily reflect specific free energies of reaction (23). In our work, tissue surface tensiometry was developed as a means for measuring the intensities of fully matured intercellular adhesions within tissue-like aggregates of motile cells under physiological conditions and at conformational equilibrium (10–12). Equally rigorous thermodynamic methods do not yet exist for measuring the free energies of

binding between cells and extracellular substrata. We therefore have used two different assays to reveal differences in the adhesiveness of our engineered L cell lines to the synthetic substrata. A distractive method, in which inversion of the substratum applies a distractive force of 1 *g* to the attached cells, has shown that attachments between cells and poly(DTE-co-PEG carbonate) substrata are weakened in proportion to the amount of PEG incorporated into the copolymer. Supporting that conclusion, observations of the morphology of parallel cultures have shown that as PEG content approaches 5%, cells deposited on the polymer aggregate rather than spread. These observations support our conclusion that the cells in these experiments adhere more weakly to poly(DTE-co-PEG carbonate) substrata of higher PEG content.

Regulation of tissue spreading movements by differential cellular cohesion and adhesion has been demonstrated in both embryonic morphogenesis (10–12, 24) and malignant invasion (25–27). Rate of locomotion of individual cells is strongly influenced by the cells' adhesivity to the substratum, which itself is a function of the density of extracellular ligands and their cellular receptors, ligand-receptor affinity, and other factors that modulate these adhesions or exert chemotactic influences (28–37). We demonstrate here that rate of spreading of a cell population on a substratum is influenced, in addition, by the intensity of cohesion among the cells themselves. N-cadherin has been shown to directly promote motility in breast cancer cells, perhaps through a mechanism involving fibroblast growth factor receptor signaling and matrix metalloproteinase-9 production (38, 39). However, this cannot be the mechanism through which N-cadherin has influenced aggregate spreading in the present experiments with L cells, as spreading would in that case have been increased rather than decreased by N-cadherin expression.

In the emerging field of tissue engineering, the importance of cell–cell cohesivity in determining the ability of cells to spread over an implanted scaffold has not previously been demonstrated. Recognition of the interplay between a tissue's adhesion to a substratum and its cohesion may contribute to the rational design of scaffold materials. These materials might be designed, for example, to favor the adhesion and spreading of desired cell types or to release, for a limited time period, inhibitors of cell–cell cohesion that would speed tissue spreading over the scaffold.

We thank Masatoshi Takeichi for the pMiwcN-cadherin vector, Louis Reichardt for the L929 R-cadherin transfected cell line, Duke Duguay for measurement of LR1 cell aggregate surface tension, Joseph Goodhouse for assistance with confocal imaging, and Prabhas Moghe and Carolyn Cho for helpful comments. This work was supported by Grant HD30345 from the National Institute of Child Health and Human Development, National Institutes of Health to M.S.S., Grant GM39455 from the National Institute of General Medical Sciences, National Institutes of Health to J.K., by the New Jersey Center for Biomaterials through an R&D Excellence Award from the New Jersey Commission on Science and Technology, and by ConvaTec Inc.

1. Martz, E., Phillips, H. M. & Steinberg, M. S. (1974) *J. Cell. Sci.* **16,** 401–419.
2. Yu, C. & Kohn, J. (1999) *Biomaterials* **20,** 253–264.
3. Pulapura, S. & Kohn, J. (1992) *Biopolymers* **32,** 411–417.
4. Ertel, S. I. & Kohn, J. (1994) *J. Biomed. Mater. Res.* **28,** 919–930.
5. Hooper, K. A., Macon, N. D. & Kohn, J. (1998) *J. Biomed. Mater. Res.* **41,** 443–454.
6. Inuzuka, H., Miyatani, S. & Takeichi, M. (1991) *Neuron* **7,** 69–79.
7. Murphy-Erdosh, C., Yoshida, C. K., Paradies, N. & Reichardt, L. F. (1995) *J. Cell. Biol.* **129,** 1379–1390.
8. Miyatani, S., Shimamura, K., Hatta, M., Nagafuchi, A., Nose, A., Matsunaga, M., Hatta, K. & Takeichi, M. (1989) *Science* **245,** 631–635.
9. Fujimori, T., Miyatani, S. & Takeichi, M. (1990) *Development (Cambridge, U.K.)* **110,** 97–104.
10. Foty, R. A., Pfleger, C. M., Forgacs, G. & Steinberg, M. S. (1996) *Development (Cambridge, U.K.)* **122,** 1611–1620.
11. Foty, R. A., Forgacs, G., Pfleger, C. M. & Steinberg, M. S. (1994) *Phys. Rev. Lett.* **72,** 2298–2301.
12. Davis, G. M., Phillips, H. M. & Steinberg, M. S. (1997) *Dev. Biol.* **192,** 630–644.
13. Steinberg, M. S. (1996) *Dev. Biol.* **180,** 377–388.
14. Tziampazis, E., Kohn, J. & Moghe, P. V. (2000) *Biomaterials* **21,** 511–520.
15. Coman, D. R. (1944) *Cancer Res.* **4,** 625–629.
16. McClay, D. R., Wessel, G. M. & Marchase, R. B. (1981) *Proc. Natl. Acad. Sci. USA* **78,** 4975–4979.
17. Angres, B., Barth, A. & Nelson, W. J. (1996) *J. Cell. Biol.* **134,** 549–557.
18. Steinberg, M. S. (1964) in *Cellular Membranes in Development*, ed. Locke, M. (Academic, New York), pp. 321–366.
19. Evans, E., Berk, D. & Leung, A. (1991) *Biophys. J.* **59,** 838–848.
20. Roth, S. A. & Weston, J. A. (1967) *Proc. Nat. Acad. Sci. USA* **58,** 974–980.
21. Roth, S. A. (1968) *Dev. Biol.* **18,** 602–631.
22. Nose, A., Nagafuchi, A. & Takeichi, M. (1988) *Cell* **54,** 993–1001.
23. Glasstone, S., Laidler, K. J. & Eyring, H. (1941) *The Theory of Rate Processes: The Kinetics of Chemical Reactions, Viscosity, Diffusion, and Electrochemical Phenomena* (McGraw–Hill, New York).
24. Davis, G. S. (1984) *Am. Zool.* **24,** 649–655.
25. Ziober, B. L., Lin, C. S. & Kramer, R. H. (1996) *Semin. Cancer Biol.* **7,** 119–128.
26. Bracke, M. E., Van Roy, F. M. & Mareel, M. M. (1996) *Curr. Top. Microbiol. Immunol.* **21,** 123–161.
27. Foty, R. A. & Steinberg, M. S. (1997) *Cancer Res.* **57,** 5033–5036.
28. Bauer, J. S., Schreiner, C. L., Giancotti, F. G., Ruoslahti, E. & Juliano, R. L. (1992) *J. Cell. Biol.* **116,** 477–487.
29. DiMilla, P. A., Stone, J. A., Quinn, J. A., Albelda, S. M. & Lauffenburger, D. A. (1993) *J. Cell. Biol.* **122,** 729–737.
30. Duband, J. L., Dufour, S., Yamada, S. S., Yamada, K. M. & Thiery, J. P. (1991) *J. Cell. Sci.* **98,** 517–532.
31. Giancotti, F. G. & Ruoslahti, E. (1990) *Cell* **60,** 849–859.
32. Huttenlocher, A., Ginsberg, M. H. & Horwitz, A. F. (1996) *J. Cell. Biol.* **134,** 1551–1562.
33. Huttenlocher, A., Sandborg, R. R. & Horwitz, A. F. (1995) *Curr. Opin. Cell. Biol.* **7,** 697–706.
34. Keely, P. J., Fong, A. M., Zutter, M. M. & Santoro, S. A. (1995) *Cell. Sci.* **108,** 595–607.
35. Lauffenburger, D. A. & Horwitz, A. F. (1996) *Cell* **84,** 359–369.
36. Palecek, S. P., Loftus, J. C., Ginsberg, M. H., Lauffenburger, D. A. & Horwitz, A. F. (1997) *Nature (London)* **385,** 537–540.
37. Kassner, P. D., Alon, R., Springer, T. A. & Hemler, M. E. (1995) *Mol. Biol. Cell.* **6,** 661–674.
38. Nieman, M. T., Prudoff, R. S., Johnson, K. R. & Wheelock, M. J. (1999) *J. Cell. Biol.* **147,** 631–644.
39. Hazan, R. B., Phillips, G. R., Qiao, R. F., Norton, L. & Aaronson, S. A. (2000) *J. Cell. Biol.* **148,** 779–790.